Journal of Environmental Chemical Engineering 4 (2016) 3688–3695

Contents lists available at ScienceDirect

Journal of Environmental Chemical Engineering

journal homepage: www.elsevier.com/locate/jece

Methane dry reforming using Ni/Al_2O_3 catalysts: Evaluation of the effects of temperature, space velocity and reaction time

Carine Aline Schwengber[a,b], Fernando Alves da Silva[c], Rodolfo Andrade Schaffner[a], Nadia Regina Correia Fernandes-Machado[c], Ricardo José Ferracin[b], Vanessa Rossato Bach[a,b], Helton José Alves[a,b,*]

[a] Laboratory of Catalysis and Biofuel Production (LabCatProBio), Federal University of Paraná (UFPR), R. Pioneiro, 2153, 85950-000, Palotina, PR, Brazil
[b] Postgraduate Program in Bioenergy, Federal University of Paraná (UFPR), R. Pioneiro, 2153, 85950-000, Palotina, PR, Brazil
[c] Department of Chemical Engineering, State University of Maringá (UEM), Av. Colombo, 5790, 87020-900, Maringá, PR, Brazil

ARTICLE INFO

Article history:
Received 28 March 2016
Received in revised form 2 June 2016
Accepted 1 July 2016
Available online 1 July 2016

Keywords:
Catalytic reforming
Biogas
Methane
Carbon dioxide
Hydrogen

ABSTRACT

In this study, 15% Ni/Al_2O_3 and 30% Ni/Al_2O_3 catalysts were prepared by the wet impregnation method and characterized by flame atomic absorption spectrometry (FAAS) (metal content), N_2 physisorption, temperature programmed reduction (TPR), X-ray diffraction (XRD) and temperature programmed desorption of ammonia (TPD-NH_3). A continuous flow tubular reactor was built to perform the catalytic reaction tests, and the following reaction variables were analyzed: reaction temperature (600–700 °C range), space velocity (WHSV of 15 and 45 L h^{-1} g_{cat}−1) and reaction time (up to 10 h). Increasing the reaction temperature in the dry reforming reactions led to higher H_2 yields and higher conversions of CH_4 and CO_2. In general, better conversion rates were achieved in the reactions performed with the 15% Ni/Al_2O_3 catalyst. In the reactions in which the space velocity was varied, it was observed that increasing the space velocity (WHSV of 45 L h^{-1} g_{cat}^{-1}) decreased CH_4 conversion so the reaction rate is also controlled by the bed length and hence favored the dry reforming reaction. The results of the reaction tests performed for 10 h indicated that no significant loss of catalytic activity occurred during the reaction, therefore no deactivation occurred by coke deposition or metal sintering.

1. Introduction

Concern for the environment and the search for alternative energy sources have led to the development of technologies aimed at economic development coupled with minimization of environmental impacts. An ideal energy source is one that is inexpensive, clean, renewable and sustainable. One such source energy that is promising is biogas produced by the anaerobic decomposition of plant and animal wastes, typically composed of 55–75% methane (CH_4) and 25–44% carbon dioxide (CO_2), associated with traces of other gases such as hydrogen sulfide (H_2S), ammonia (NH_3), hydrogen (H_2), nitrogen (N_2), oxygen (O_2) and water vapor (H_2O) [1–4].

Methane reforming with CO_2 is a relevant process from the environmental standpoint because CO_2, one of the gases responsible for the greenhouse effect, can be converted, together with CH_4, into H_2 and CO (Eq. (1)) [5,6]. This process is endothermic, thus requiring high temperatures and with low pressures. In general, dry reforming (DR) takes place at temperatures varying from 600 to 900 °C, using a CH_4/CO_2 molar ratio of 1–1.5 to obtain H_2 yields of about 50% [6–9].

$$CH_4 + CO_2 \leftrightarrow 2CO + 2H_2 \qquad \Delta H_{298} = +247.0\ kJ/mol \qquad (1)$$

The main reaction may be accompanied by parallel reactions such as reverse water-gas shift (Eq. (2)), methanation (Eq. (3)), carbon monoxide decomposition by the Boudouard reaction (Eq. (4)), the undesired methane decomposition reaction (Eq. (5)), and also CO reduction (Eq. (6)) [1,10].

$$CO + H_2O \leftrightarrow CO_2 + H_2 \qquad \Delta H_{298} = -41.0\ kJ/mol \qquad (1)$$

* Corresponding author at: Postgraduate Program in Bioenergy, Federal University of Paraná (UFPR), R. Pioneiro, 2153, 85950-000, Palotina, PR, Brazil.
E-mail addresses: helquimica@gmail.com, helton.alves@ufpr.br (H.J. Alves).

http://dx.doi.org/10.1016/j.jece.2016.07.001
2213-3437/

$$CO_2 + 4H_2 \leftrightarrow CH_4 + 2H_2O \qquad \Delta H_{298} = +165.0\ kJ/mo \tag{2}$$

$$2CO \leftrightarrow C + CO_2 \qquad \Delta H_{298} = -172.0\ kJ/mol \tag{3}$$

$$CH_4 \leftrightarrow C + 2H_2 \qquad \Delta H_{298} = +75.0\ kJ/mol \tag{4}$$

$$CO + H_2 \leftrightarrow C + H_2O \qquad \Delta H_{298} = -131.0\ kJ/mol \tag{5}$$

One of the main problems of the DR process is the coke formation. To minimize coke formation, it requires adjustments the process parameters such as temperature, flow rate, support and active phase [6,8,11].

Nickel based alumina catalysts (Ni/Al_2O_3) have been recognized as the most effective materials for methane reforming reactions, due to their low cost and high activity [5,6,9]. Although several studies have focused on this type of catalyst, few of them have correlated the reaction variables with H_2 production efficiency.

Therefore, the purpose of this study was to perform methane reforming in the presence of carbon dioxide, using Ni/Al_2O_3 catalysts with different mass contents of Ni, and to evaluate the influence of reaction variables (temperature, space velocity and reaction time) on hydrogen production.

2. Materials and methods

2.1. Preparation of the catalysts

The Ni/Al_2O_3 catalysts with metal loading of 15% and 30% weight were obtained by wet impregnation with an aqueous solution of nickel nitrate hexahydrate [$Ni(NO_3)_26H_2O$] (Sigma-Aldrich) on a commercial Al_2O_3 support. After impregnation in a rotary evaporator, the catalyst was oven-dried at 110 °C for 24 h. The material was ground into particles of approximately 0.05 mm, and then calcined under the following conditions: at 3.0 °C min^{-1} from room temperature to 200 °C/60 min; followed by 500 °C/60 min, and at 5.0 °C min^{-1} up to 800 °C/4 h.

2.2. Characterization of the catalysts

The metal content was quantified by flame atomic absorption spectrometry (FAAS) (Varian SpectrAA 50). The textural analysis was performed on N_2 isotherms, using a Quantachrome Instruments NOVA 2000e surface area analyzer.

The crystalline phases were analyzed qualitatively by X-ray diffraction (XRD) using a Shimadzu Lab XRD-6000 X-ray diffractometer, at a 2θ angle between 5° and 70°, with CuKα radiation (λ = 1.5406 Å), operating at 40 kV, 30 mA, and a continuous scanning rate of 1.5°/min.

Temperature programmed desorption of ammonia (TPD-NH_3) was performed in a Quantachrome Instruments ChemBET 3000 multipurpose unit equipped with a thermal conductivity detector to verify the acid strength of active sites in the samples. About 100 mg of sample was placed in the unit and pretreated for 60 min at a temperature of 300 °C under nitrogen at a flow rate of 30 mL min^{-1}. Then, samples were reduced under with 30 mL/min of 5% H_2/N_2 mixture flow, followed by ammonia adsorption at 100 °C. After adsorption, the physisorbed portion was purged with N_2 gas, followed by desorption of chemisorbed NH_3 at a rate of 10 °C min^{-1} up to 700 °C.

For the temperature program reduction, samples were submitted to a 1.75% H_2/Ar mixture flow of 30 mL/min, with a 10 °C/min heating rate from room temperature until 1000 °C. The outlet gas was analyzed by a TCD, so the H_2 consumed by the catalyst could be accomplished.

2.3. Catalytic tests

A methane dry reforming system was built (see Fig. 1) and it consists in four gas cylinder with manometers for pressure regulation. All tubes used in the system are 314 stainless still $^1/_4$ in. All gases pass through the regulator system (1), where inlet pressure and flow can be controlled. The tube-reactor connections are quick-coupler. Gases are mixture in a gas camera of 250 mL internal volume, where the inlet flow cross a single-pass valve (2), so gases still flow in only one direction. After that, the mixture flow comes in an electric pre-furnace (5) for previous heating; here, 6 m of tube is used to guarantee the temperature condition. Then, the reaction mixture goes to the reforming furnace (6) and so the tubular U-shaped reactor (7), where the reaction begins. Digital controllers are used in the pre-furnace and reactor to reach the

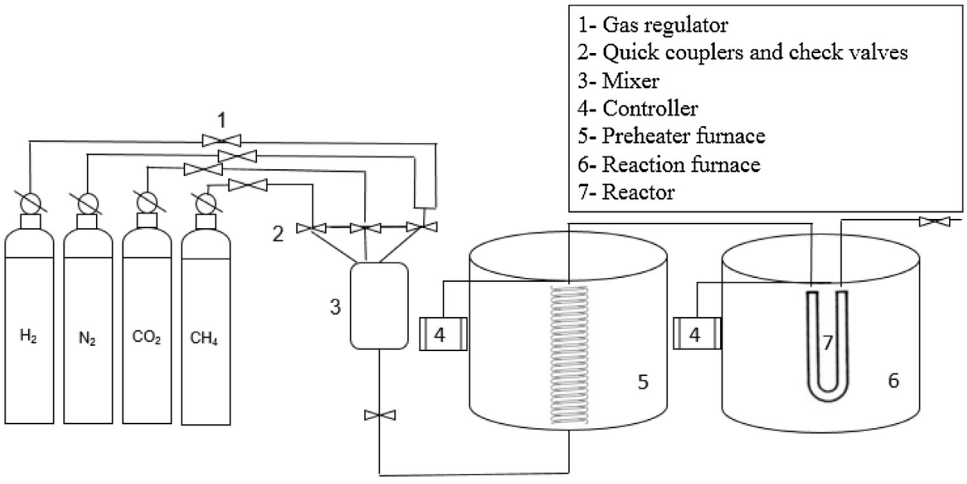

Fig. 1. Schematic diagram of the reactor used for methane dry reforming.

necessary power, and each one has K thermocouple for temperature control. The outlet gas flow is monitored using a glass flow system control.

The catalyst was activated *in situ* in all the tests, using a H_2 flow of 40 mL min^{-1} for 10 h at the reaction temperature. After that, N_2 flow was used for previous inert conditions.

First, the catalytic tests were conducted with constant space velocity (WHSV- reactants flow per mass of catalyst) at 30 L. h^{-1} $g_{cat}{}^{-1}$ with a fixed amount of 300 mg of catalyst and a CO_2:CH_4 molar ratio of 1, at temperatures of 600, 650 and 700 °C, for the 15% Ni/Al_2O_3 and 30% Ni/Al_2O_3 catalysts. Then, tests were performed with different WHSV (15 and 45 L h^{-1} $g_{cat}{}^{-1}$) and mass of catalyst (600 and 200 mg), a temperature of 650 °C and reaction time of 4 h. For the long during tests, reaction time was extended up to 10 h.

The gas product was analyzed in an Agilent 7890A gas chromatograph equipped with a TCD detector.

3. Results and discussion

3.1. Characterization of the catalysts

Table 1 lists the N_2 physisorption results obtained for the catalysts after calcination and for non-calcined alumina. Fig. 2 shows the N_2 adsorption and desorption isotherms.

It was found that the specific surface area of the impregnated materials decreased in relation to the support, as a result of the impregnation of Ni in the pores and on the surface of alumina. According to IUPAC (1976) [12], the isotherms of the materials can be classified as type IV, which is characteristic of mesoporous solids (pores with average diameter of 20 Å < Ø ≤ 500 Å).

Table 1 shows that the average pore diameters ranged from 70 to 115 Å, indicating that the catalysts are mesoporous. The graph in Fig. 3 shows the pore size distribution according to the BJH model.

Table 1
Textural properties of the catalyst and support.

Sample	S_{BET} ($m^2 g^{-1}$)	Pore size/volume ($cm^3 g^{-1}$) (BJH)	Mean pore diameter (Å) (BJH)
Al_2O_3	200	0.63	72.9
15% Ni/Al_2O_3	143	0.68	114.9
30% Ni/Al_2O_3	118	0.48	114.0

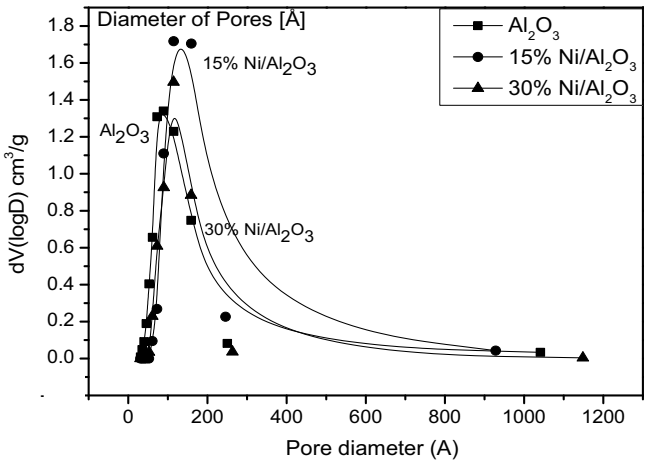

Fig. 3. Pore size distribution after desorption (dV(logD)cm^3/g) of non-calcined AL_2O_3, and 15% $NiAl_2O_3$ and 30% $NiAl_2O_3$ catalysts calcined at 800 °C.

It was noted monomodal pore volume distribution of the materials, with well-defined maximum distribution.

The reduction on surface area was attributed to the active phase in the internal porous, which causes pore blocking; so, no NiO diffraction peaks could be observed in the diffractogram of the catalysts, as it can be seen in Fig. 4. There was an increase on the crystallinity of the catalysts compared to pure support. It was not identified changes on support phase crystallinity; the $NiAl_2O_4$ formation in the same theta position of some Al_2O_3 diffraction peaks revealed a great active phase dispersion and strong metal support interaction (SMSI) [13]. This oxide, although the low reducibility to metallic Ni, is favourable on high thermal reaction since no sinterization can took place.

Although no NiO diffraction peak was found on the XRD diffractograms, the TPR profiles showed different oxides in each catalyst (Fig. 5), both with high interaction with the support.

Two H_2 consumption peaks were detected in the catalysts with different Ni contents (Fig. 5). The first peak of the 15% Ni/Al_2O_3

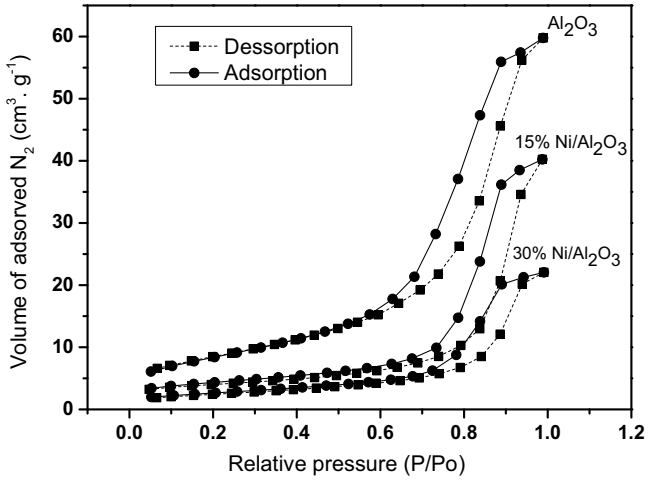

Fig. 2. N_2 adsorption/desorption isotherms of non-calcined Al_2O_3, and of 15% Ni/Al_2O_3 and 30% Ni/Al_2O_3 catalysts calcined at 800 °C.

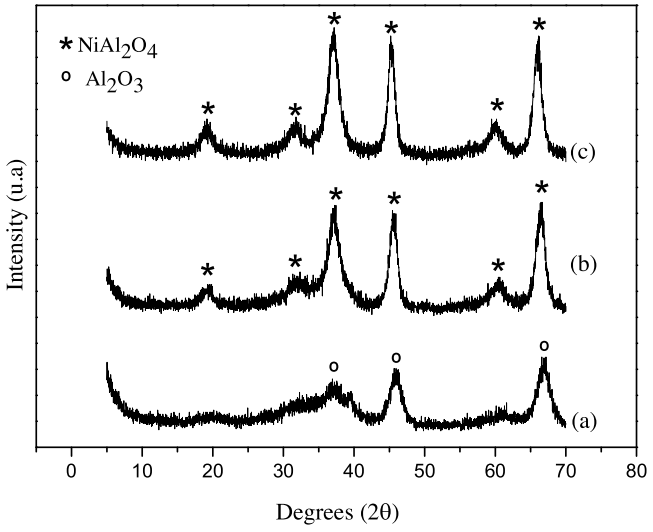

Fig. 4. XRD patterns of (a) non-calcined Al_2O_3, (b) 15% Ni/Al_2O_3 calcined at 800 °C, and (c) 30% Ni/Al_2O_3 calcined at 800 °C.

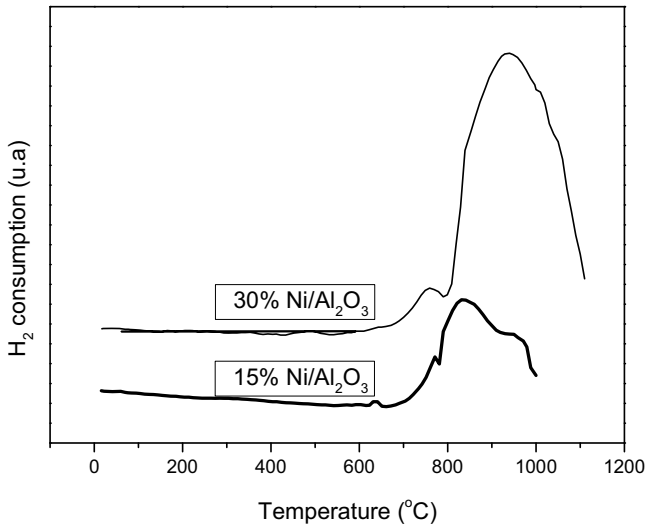

Fig. 5. TPR profiles of the 15% $NiAl_2O_3$ and 30% $NiAl_2O_3$ catalysts calcined at 800 °C.

Table 2
Acidity (TPD-NH_3).

	Al_2O_3	15% Ni/Al_2O_3	30% Ni/Al_2O_3
Desorbed ammonia (mmol NH_3/g)	0.074	0.039	0.038
Decreased acidity[a]	–	52.70%	51.35%

[a] In relation to the Al_2O_3 support.

catalyst appeared at 631 °C and the second at 831 °C. The first peak of the 30% Ni/Al_2O_3 catalyst appeared at 759 °C and the last at 940 °C, indicating that an increase in the nickel composition did not altered the formation of oxides. The first peak in both catalysts may be attributed to NiO species of small sizes unidentified by XRD, dispersed in the alumina matrix, while the last peak may indicate the reduction of nickel oxide with more interaction with the support, probably the $NiAl_2O_4$ phase identified by XRD [14]. The 15% Ni/Al_2O_3 catalyst showed a slight reduction, indicating that the reduction of the oxide with the highest interaction occurred in two steps. The interaction between metal and support was more intense in the last peak, where the nickel reduction temperature was higher.

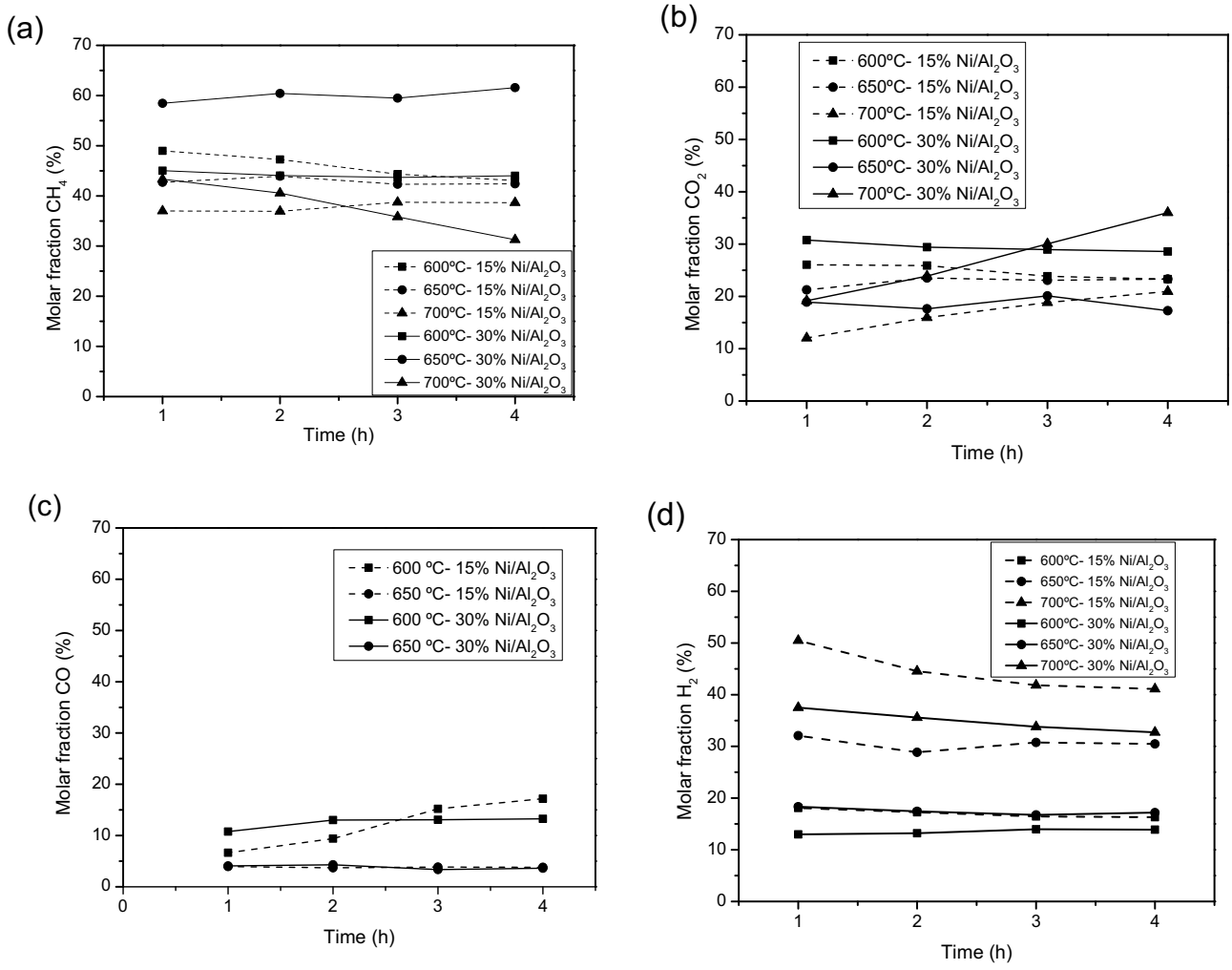

Fig. 6. Molar fraction of products obtained at WHSV = 30 L h^{-1} g_{cat}^{-1} at different temperatures: (a) CH_4; (b) CO_2 (c) CO, and (d) H_2.

The analysis of TPD-NH_3 indicated two desorption peaks of the alumina support, with the maximum desorption temperature of the first peak at 206 °C attributed to weak acid sites and the maximum temperature of the second peak at 459 °C attributed to stronger acid sites. The incorporation of Ni on alumina led to the formation of an ammonia desorption peak in both catalysts: one at 269 °C for the 15% Ni/Al_2O_3 catalyst and the other at 335 °C for the 30% Ni/Al_2O_3 catalyst. Table 2 shows the quantification of the acid sites.

The addition of Ni reduced the acidity and led to the formation of only one NH_3 desorption peak. The reduction to a single ammonia desorption peak suggests that the incorporation of the metal occurred preferentially at one type of acid site, causing this group to become coated. The decrease in acidity favors the stability of the catalyst, reducing the deposition of carbon and preventing its deactivation [6].

3.2. Catalytic tests in methane dry reforming

Fig. 6 illustrates the results of the molar fraction of the gas product obtained in the tests in the range of temperatures.

In Fig. 6, note that at the temperature of 650 °C the 30% Ni/Al_2O_3 catalyst presented a higher percentage of CH_4 (average of 59%), followed by the reaction performed at 600 °C. In the other experiments, the percentage of CH_4 was found to fall within the range of 30–40%. These results showed that not only complete dry reforming occurred, but also other undesired reactions, so the no-stoichiometric conversion was reached.

The highest percentage of H_2 (d) was obtained at 700 °C, where the first hour of reaction yielded values of 50 and 38% for the 15% Ni/Al_2O_3 and 30% Ni/Al_2O_3 catalysts, respectively. However, in the fourth hour of reaction, the molar fraction of H_2 dropped down to 41 and 32% for the same order catalysts, which may be attributed to the higher rate of coke formation at this temperature. In addition, the percentage of CO_2 (b) at 700 °C was found to increase over time-on-stream, indicating that the deactivation rate of the catalyst at 700 °C was higher than the other catalysts. The formation of CO (c) was observed at lower temperatures, and at 600 °C the 15% Ni/Al_2O_3 catalyst showed a CO molar fraction of 7–18% in the time range evaluated, while the 30% Ni/Al_2O_3 catalyst varied from 10 to 13%. At 650 °C, the catalysts presented an average of 3.82% of CO.

The results suggested the occurrence of parallel reactions, such as the water-gas shift reaction (Eq. (2)), in which CO reacts with H_2O to form CO_2 and H_2, and the Boudouard reaction (Eq. (4)). Another parallel reaction was the reduction of CO (Eq. (6)) by H_2, forming C and H_2O. In general, increasing the load of Ni metal resulted in a lower conversion of the reactants (Fig. 7) at the same temperature, indicating that the parallel reactions occurred more effectively, so the molar fractions of the products was farther from the stoichiometric proportions. The increase in nickel loading led to the formation of larger crystallite sizes, and hence less dispersion, which is unfavorable for the conversion of reagents.

Besides, in cases where the H_2/CO ratio was higher than 1, the selectivity for CO_2 was higher than for CO. This fact may be attributed to the formation of water vapor, which in turn, may be consumed in the process, reducing the percentage of CO through the water-gas shift reaction (Eq. (2)) [15]. Fig. 7 depicts the CH_4 and CO_2 conversions.

The conversion profiles in Fig. 7 indicated that, in general, the 15% Ni/Al_2O_3 catalyst showed a higher reactant conversion rate. This higher conversion was attributed to the lower metal load, which favors metal dispersion, reduces the occupation of acid sites in alumina, and it facilitates oxide reduction, as observed in the TPR, thus increasing the conversion rate. Furthermore, the

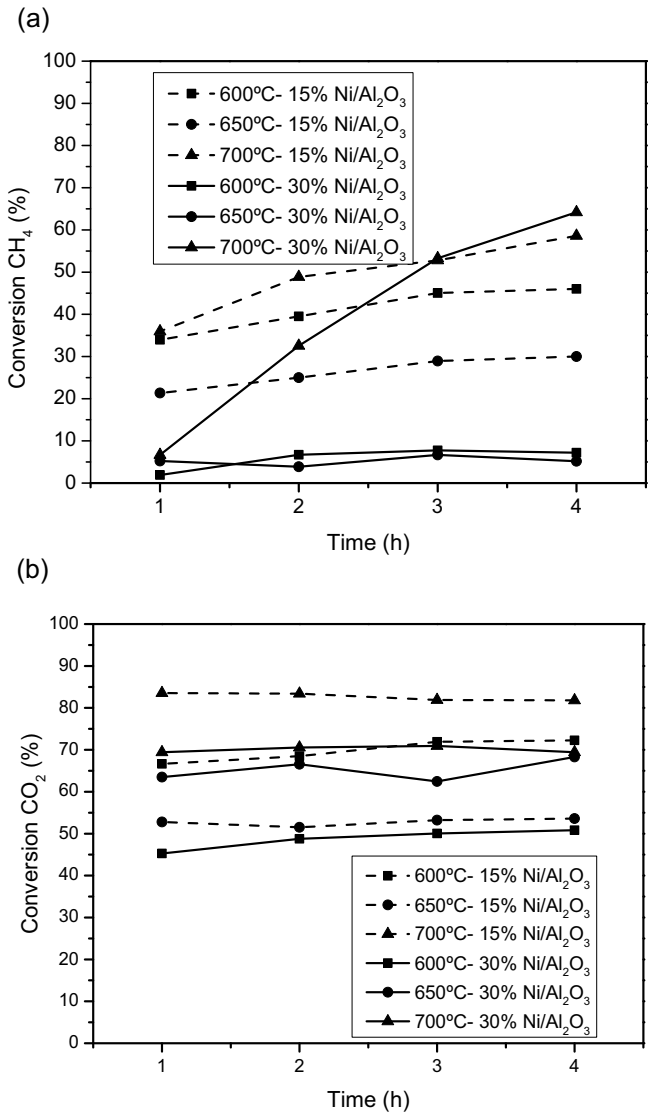

Fig. 7. Conversion of (a) CH_4 and (b) CO_2 at different temperatures, using WHSV = 30 L h^{-1} g_{cat}^{-1}.

lower metallic loading reduced the reaction rate and hence, lower coke deposition took place at Ni sites, since this is favourable to occur in that metal. The 15% Ni/Al_2O_3 catalyst presented a CH_4 (a) conversion rate of 36–59% at 700 °C, 21–30% at 650 °C, and 34–46% at 600 °C. In reactions with the 30% Ni/Al_2O_3 catalyst at 600 and 650 °C, the CH_4 conversion rate varied from 2% to 8%, suggesting that the methanation reaction (Eq. (2)) occurred [16].

The highest CO_2 conversions (b) occurred in the reactions at 700 °C (15% Ni/Al_2O_3, conversion of 80–84%, and 30% Ni/Al_2O_3, conversion of 69–71%), followed by the reactions of the 15% Ni/Al_2O_3 catalyst at 600 °C (66–73%) and at 650 °C (51–54%).

The surface CH_4 decomposition in Ni sites was attributed as the main deactivation mechanism since led to coke formation. Then, the decrease in CO_2 adsorption for the C gasification resulted in higher CH_4 conversion than CO_2. This contributed for the increase on H_2 selectivity even without higher CO production [8,17].

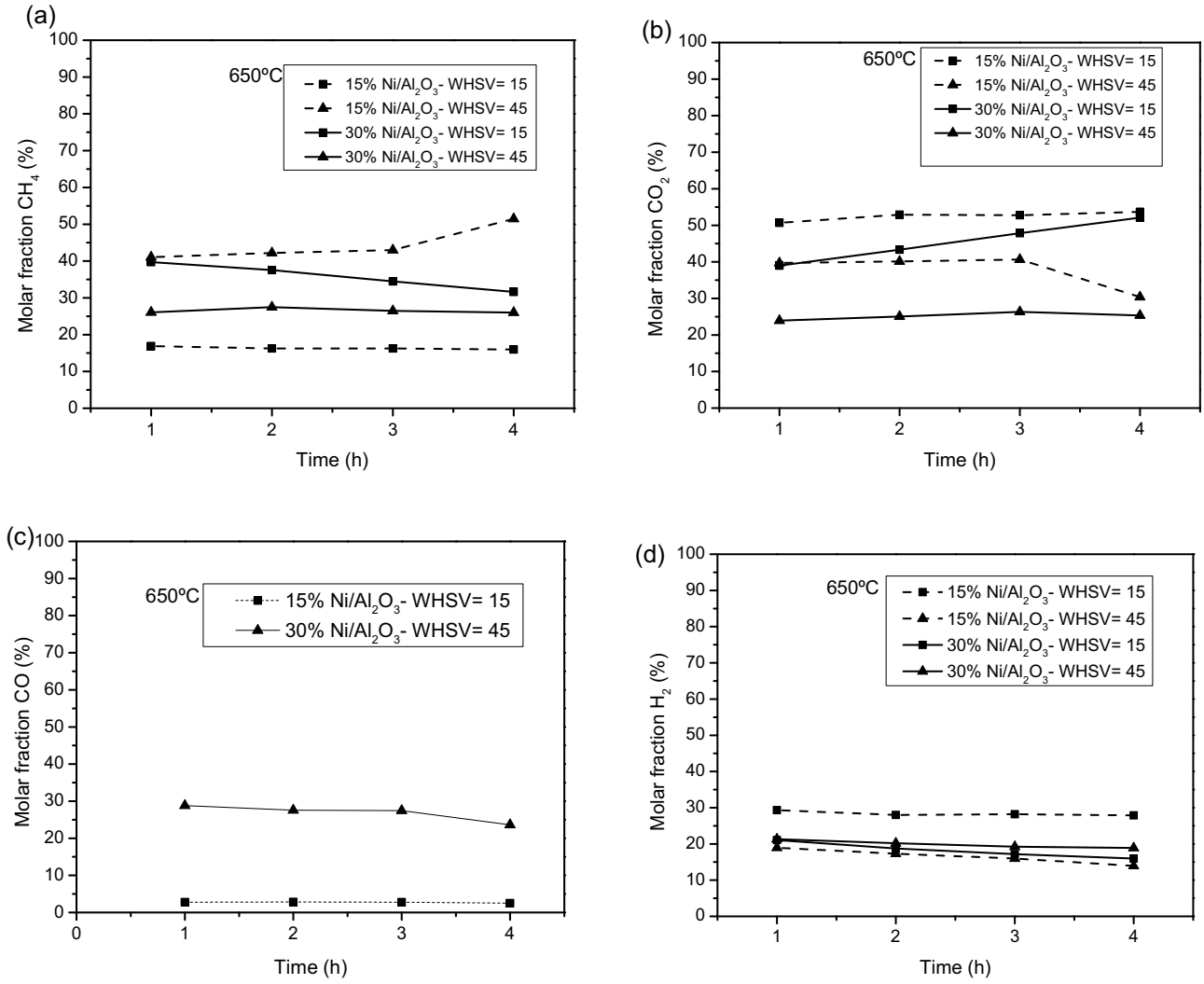

Fig. 8. Molar fractions at 650 °C, with different WHSV values ($L\,h^{-1}\,g_{cat}^{-1}$): (a) CH_4; (b) CO_2; (c) CO; and (d) H_2.

The temperature of 650 °C was chosen for the tests with different WHSV values, since the reactions at 700 °C showed an increase in coke formation that partially obstructed the reactor. Fig. 8 illustrates the molar fractions of the products of the reactions at 650 °C with different space velocities (WHSV of 15 and 45 $L\,h^{-1}\,g_{cat}^{-1}$).

The highest molar fractions of H_2 (d) (27–30%) were obtained in the test with the 15% Ni/Al_2O_3 catalyst at a WHSV of 15 $L\,h^{-1}\,g_{cat}^{-1}$.

The larger H_2 selectivity was reached for this catalyst with lower metal loading, which is in accordance with the catalyst properties and the dry reforming mechanism. The nickel dispersion favored CH_4 decomposition and C gasification. Then, no completely deactivation occurred for that catalyst. This reaction mechanism also explains the absence of CO since no adsorbed C underwent its gasification [18].

The formation of CO (d) (2–3%) occurred only in the test with 15% Ni/Al_2O_3 using a WHSV of 15 $L\,h^{-1}\,g_{cat}^{-1}$ and in the test with 30% Ni/Al_2O_3 (26–28%) using a WHSV of 45 $L\,h^{-1}\,g_{cat}^{-1}$. Fig. 9 shows the CH_4 and CO_2 conversion rates (%) at different space velocities.

The conversion profile for CH_4 pointed out for decreasing conversion with increasing the WHSV, for the same catalyst. This was expected cause the lower flow residence time. On the other side, for the same WHSV, the increase on nickel loading led to lower reaction rate, which was attributed to the quick catalyst deactivation. For the 15% Ni/AL_2O_3 with WHSV = 15 $L\,h^{-1}\,g_{cat}^{-1}$, the increase on CH_4 conversion respect to time-on-stream indicated a constant product desorption and no deactivation.

The results indicated that a larger amount of catalyst (lowest space velocity) in the reaction bed favored CH_4 conversion. In general, larger WHSV was desfavorable for CH_4 conversion since small bed length was used, and that was also observed by Rahemi et al. [18].

For CO_2, an opposite behavior was presented in Fig. 9. The increase on WHSV favored its conversion using the 15% Ni/Al_2O_3 catalyst. This revealed that CO_2 is not consumed in the final elementary steps of the reaction, since the adsorption and

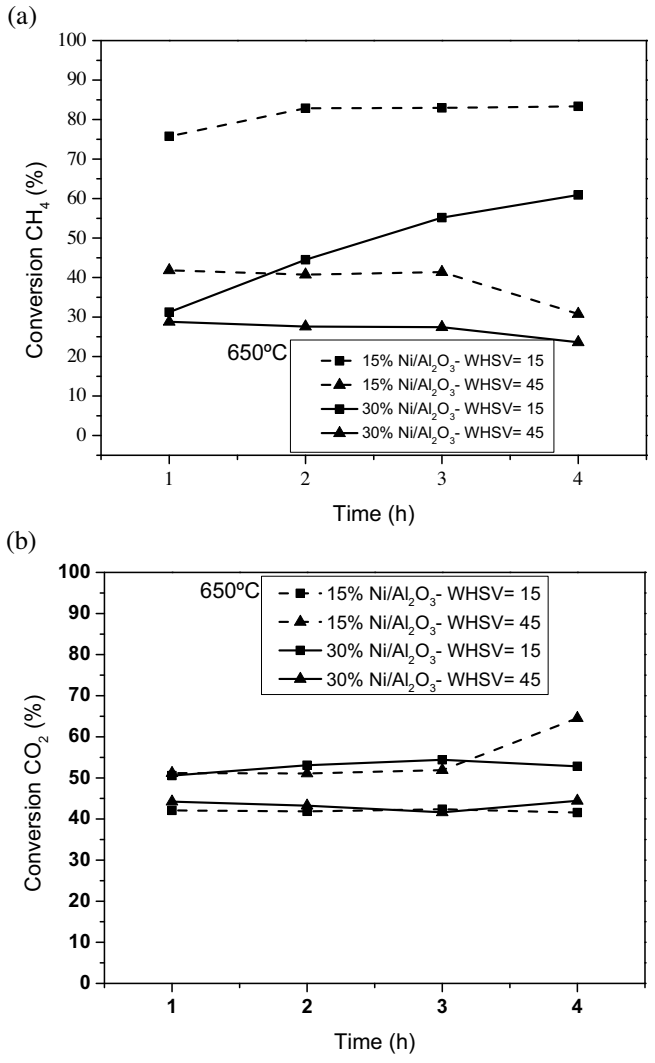

Fig. 9. Conversion of (a) CH_4 and (b) CO_2 at 650 °C at different WHSV ($L\,h^{-1}\,g_{cat}^{-1}$).

conversion of this reactant was further for higher WHSVs. For the 30% Ni/Al_2O_3, the same behavior was not observed. The higher nickel loading increased the CH_4 decomposition in the metal surface, and hence less active sites was free for CO_2 adsorption. So, the mechanism passed for the no-stoichiometric way and a fast deactivation from CH_4 decomposition decreased the CO_2 conversion.

Besides the mechanism and catalyst properties, it is important to consider that all involved reactions in the dry reforming process (i.e. water gas shift reaction, for example) could reach – or not – the thermodynamic equilibrium. Fig. 10 indicates the reactants conversion in the temperature range for both 15 and 30% Ni/Al_2O_3 catalyst.

Since a maximum on CH_4 conversion was observed for 15% Ni/Al_2O_3 catalyst, there is evidence of thermodynamic due to kinetic controlling process. For the another one, 30% Ni/Al_2O_3 did not reach the equilibrium conversion, so the progressive increase on conversion with temperature; in this case, the surface properties of the catalyst, as probably higher crystallite sizes, could reduce the reaction rate far from the equilibrium conditions. On the other side, a minimum on CO_2 conversion was observed at 650 °C, which indicates that the water gas shift reaction equilibrium could be reached, so all the CO content formed during the reaction was converted to CO_2 and led the small conversion. In fact, here, CO_2 was formed again in the process. At 750 °C, the CO_2 conversion raised up and no CO in the outlet gas composition was attributed principally to the Boudouard pathway. This occasioned a blocking on the flow through the reactor.

To evaluate the stability of the catalysts, two randomly chosen reactions were performed for 10 h, and the results are shown in Fig. 11.

Fig. 11 presents the molar fractions and conversion of the components of the gas products from the reactor during the 10 h reaction-on-stream for the 15% and 30% Ni/Al_2O_3 catalysts. Both reactions remained stable during the 10 h of reaction, which indicated no significant loss of catalytic activity during the process. This stability can be attributed to the lower strength of the active sites, and to the presence of the $NiAl_2O_4$ phase, which indicates the high metal/support interaction, hindering metal sintering.

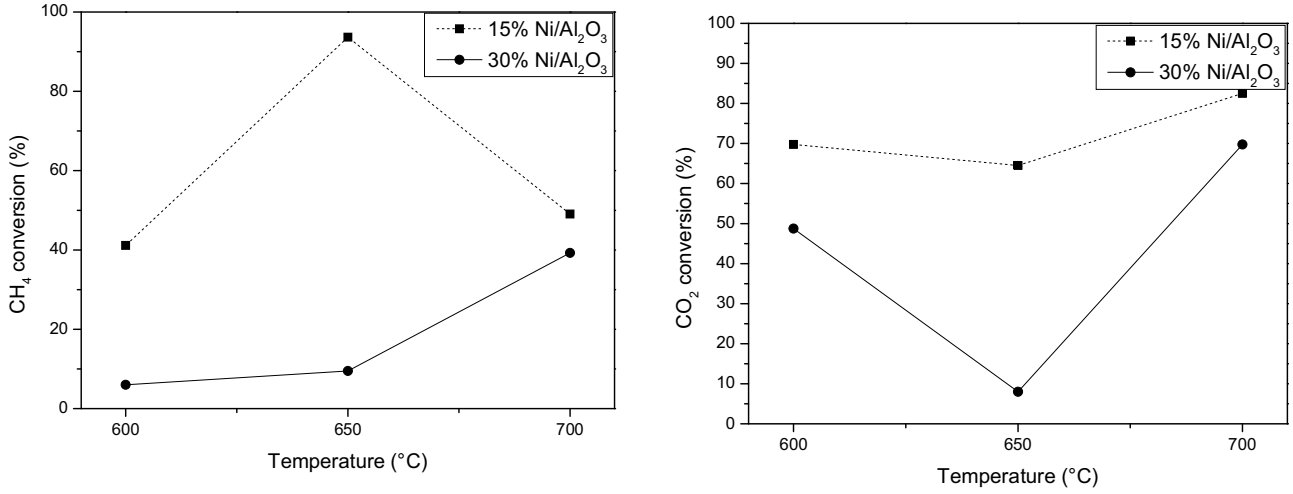

Fig. 10. CH_4 (a) and CO_2 (b) conversion at 600–700 °C range.

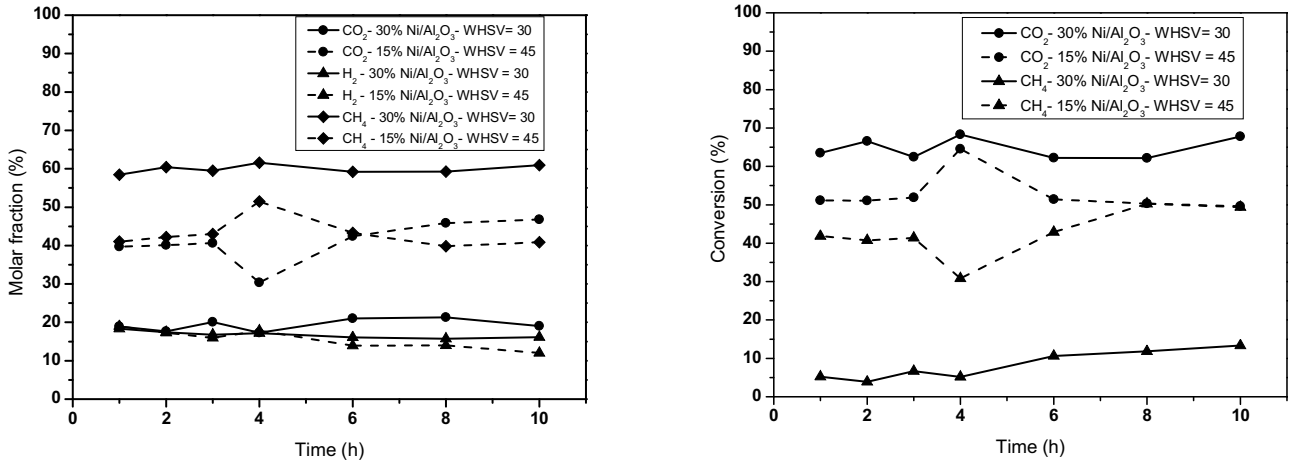

Fig. 11. Monitoring of the reactions at 650 °C for 10 h—15% Ni/Al_2O_3 and 30% Ni/Al_2O_3 catalysts.

4. Conclusions

In the dry reforming reactions, the increase on reaction temperature led to higher H_2 yields and higher CH_4 and CO_2 conversion rates. Increasing the space velocity (WHSV of 45 L h^{-1} g_{cat}^{-1}) decreased the CH_4 conversion rates, indicating that a larger amount of catalyst in the catalytic bed favored the reforming reaction. In general, the highest conversion rates were observed in the reactions conducted with the catalyst with the lower metal content (15% Ni/Al_2O_3). The results of the tests in which reaction time was extended to 10 h indicated that no significant loss of catalytic activity occurred during the reaction.

Biogas can therefore be considered an important raw material for the production of H_2, since it has a low cost and renewable source composed of two gases that are harmful to the environment. Under optimized conditions, the use of low cost catalysts that are simple to obtain, such as Ni/Al_2O_3, can contribute to render the dry reforming process as one of the most promising routes for the production of hydrogen.

Acknowledgment

The authors gratefully acknowledge theItaipu Technological Park Foundation—FPTI-BR (Project No. 37/2013) for its financial support.

References

[1] H.J. Alves, C. Junior, R.R. Nicklevicz, C.H.C. Araújo, E.P. Frigo, M.S. Frigo, Overview of hydrogen production technologies from biogas and the applications in fuel cells, Int. J. Hydrogen Energy 38 (2013) 5215–5225.
[2] A.O. Bereketidou, M.A. Goula, Biogas reforming for syngas production over nickel supported on ceria-alumina catalysts, Catal. Today 195 (1) (2012) 93–100.
[3] D. Yu, J.M. Kurola, K. Lähde, M. Kymäläinen, A. Sinkkonen, M. Romantschuk, Biogas production and methanogenic archaeal community in mesophilic and thermophilic anaerobic co-digestion processes, J. Environ. Manag. 143 (2014) 54–60.
[4] S. Fathya, K. Assia, M. Hamza, Influence of inoculums/substrate ratios (ISRs) on the mesophilic anaerobic digestion of slaughterhouse waste in batch mode: process stability and biogas production, Energy Procedia 50 (2014) 57–63.
[5] H. Eltejaei, H.R. Bozorgzadeh, J. Towfighi, M.R. Omidkhah, M. Rezaei, R. Zanganeh, Methane dry reforming on Ni/Ce0.75Zr0.25O_2–$MgAl_2O_4$ and Ni/Ce0.75Zr0.25O_2-g-alumina: effects of support composition and water addition, Int. J. Hydrogen Energy 37 (2012) 4107–4118.
[6] Z. Alipour, M. Rezaei, F. Meshkani, Effect of alkaline earth promoters (MgO, CaO, and BaO) on the activity and coke formation of Ni catalysts supported on nanocrystalline Al_2O_3 in dry reforming of methane, J. Ind. Eng. Chem. 20 (2014) 2858–2863.
[7] D. Karimipourfard, S. Kabiri, M.R. Rahimpour, A novel integrated thermally double coupled configuretion for methane steam reforming, methane oxidation and dehydrogenation of propane, J. Nat. Gas Sci. Eng. 21 (2014) 134–146.
[8] M. Abdollahifar, M. Haghighi, A.A. Babaluo, Syngas production via dry reforming of methane over Ni/Al_2O_3–MgO nanocatalyst synthesized using ultrasound energy, J. Ind. Eng. Chem. 20 (2014) 1845–1851.
[9] A.S.A. Al-Fatesh, A.H. Fakeeha, A.E. Abasaeed, Effects of Selected Promoters on Ni/γ-Al_2O_3 catalyst performance in methane dry reforming, Chin. J. Catal. 32 (10) (2011).
[10] C.S. Lau, A. Tsolakis, M.L. Wyszynski, Biogas upgrade to syn-gas (H_2-CO) via dry and oxidative reforming, Int. J. Hydrogen Energy 36 (2011) 397–404.
[11] M.A. Goula, N.D. Charisiou, K.N. Papageridis, A. Delimitis, E. Pachatouridou, E.F. Iliopoulou, Nickel on alumina catalysts for the production of hydrogen rich mixtures via the biogas dry reforming reaction: influence of the synthesis method, Int. J. Hydrogen Energy 40 (2015) 9183–9200.
[12] IUPAC—International Union of Pure and Applied Chemistry (1976).
[13] Z. Xu, Y. Li, J. Zhang, L. Chang, R. Zhou, Z. Duan, Bound-state Ni species—a superior form in Ni-based catalyst for CH_4/CO_2 reforming, Appl. Catal. A Gen. 210 (2001) 45–53.
[14] L.-C. Chen, S.D. Lin, The ethanol steam reforming over Cu–Ni/SiO_2catalysts: effect of Cu/Ni ratio, Appl. Catal. B Environ. 106 (3–4) (2011) 639–649.
[15] K. Zanoteli, J.C.C. Freitas, P.R.N. Silva, Estudo de catalisadores de níquel suportados em cinza de casca de arroz na reforma de metano com dióxido de carbono visando a produção de hidrogênio e gás de síntese, Quím. Nova 37 (10) (2014) 1657–1662.
[16] S.A. Chattanathan, S. Adhikari, M. McVey, O. Fasina, Hydrogen production from biogas reforming and the effect of H_2S on CH_4 conversion, Int. J. Hydrogen Energy 39 (2014) 19905–19911.
[17] J.C. Almeida, Catalisadores Ni/BaO-Al_2O_3 e Ni/BaO-SiO_2 para Reforma do metano com CO_2. Dissertação (Mestrado em Engenharia Química), Universidade Federal de São Carlos, São Carlos, 2012 pp.116.
[18] N. Rahemi, M. Haghighi, A.A. Babaluo, S. Allahyari, M.F. Jafari, Syngas production from reforming of greenhouse gases CH_4/CO_2 over Ni–Cu/Al_2O_3 nanocatalyst: impregnated vs. plasma-treated catalyst, Energy Convers. Manag. 84 (2014) 50–59.